Materials Science and Engineering C 69 (2016) 236–246

Contents lists available at ScienceDirect

Materials Science and Engineering C

journal homepage: www.elsevier.com/locate/msec

A novel gel based on an ionic complex from a dendronized polymer and ciprofloxacin: Evaluation of its use for controlled topical drug release

Mónica C. García [a], Julio C. Cuggino [c], Clarisa I. Rosset [a], Paulina L. Páez [a], Miriam C. Strumia [b], Ruben H. Manzo [a], Fabiana L. Alovero [a], Cecilia I. Alvarez Igarzabal [b], Alvaro F. Jimenez-Kairuz [a,*]

[a] Unidad de Investigación y Desarrollo en Tecnología Farmacéutica (UNITEFA), CONICET and Departamento de Farmacia, Facultad de Ciencias Químicas, Universidad Nacional de Córdoba, Ciudad Universitaria, X5000HUA Córdoba, Argentina
[b] Instituto Multidisciplinario de Biología Vegetal (IMBIV), CONICET and Laboratorio de Materiales Poliméricos (LAMAP), Departamento de Química Orgánica, Facultad de Ciencias Químicas, Universidad Nacional de Córdoba, Ciudad Universitaria, X5000HUA Córdoba, Argentina
[c] Instituto de Desarrollo Tecnológico para la Industria Química (INTEC), CONICET, Colectora Ruta Nac. N° 168, km. 0, Pje. El Pozo, 3000 Santa Fe, Argentina

ARTICLE INFO

Article history:
Received 25 March 2016
Received in revised form 4 June 2016
Accepted 22 June 2016
Available online 23 June 2016

Keywords:
Dendronized polymer
Hydrogel
Ciprofloxacin
Polyelectrolyte-drug complexes
Drug controlled release

ABSTRACT

The development and characterization of a novel, gel-type material based on a dendronized polymer (DP) loaded with ciprofloxacin (CIP), and the evaluation of its possible use for controlled drug release, are presented in this work. DP showed biocompatible and non-toxic behaviors in cultured cells, both of which are considered optimal properties for the design of a final material for biomedical applications. These results were encouraging for the use of the polymer loaded with CIP (as a drug model), under gel form, in the development of a new controlled-release system to be evaluated for topical administration. First, DP-CIP ionic complexes were obtained by an acid-base reaction using the high density of carboxylic acid groups of the DP and the amine groups of the CIP. The complexes obtained in the solid state were broadly characterized using FTIR spectroscopy, XRP diffraction, DSC-TG analysis and optical microscopy techniques. Gels based on the DP-CIP complexes were easily prepared and presented excellent mechanical behaviors. In addition, optimal properties for application on mucosal membranes and skin were achieved due to their high biocompatibility and acute skin non-irritation. Slow and sustained release of CIP toward simulated physiological fluids was observed in the assays (*in vitro*), attributed to ion exchange phenomenon and to the drug reservoir effect. An *in vitro* bacterial growth inhibition assay showed significant CIP activity, corresponding to 38 and 58% of that exhibited by a CIP hydrochloride solution at similar CIP concentrations, against *Staphylococcus aureus* and *Pseudomonas aeruginosa*, respectively. However, CIP delivery was appropriate, both in terms of magnitude and velocity to allow for a bactericidal effect. In conclusion, the final product showed promising behavior, which could be exploited for the treatment of topical and mucosal opportunistic infections in human or veterinary applications.

1. Introduction

Hydrogels are usually defined as a crosslinked polymeric network having the capacity to hold a large amount of water within its porous structure. The water holding capacity of hydrogels is mostly ascribed to the presence of hydrophilic groups, *e.g.* amino, carboxyl and hydroxyl groups, in the polymer network [1]. Hydrogels comprise an important class of biomaterials specially used for drug delivery applications, due to their biocompatibility, good rheological and bioadhesive properties, high capacity for drug loading and modified-release behaviors. As a result, these kinds of materials are potentially suitable as drug carriers for therapeutic uses. The use of synthetic hydrogels as carriers for drug delivery has rapidly developed over the last few decades [2]. Versatile, reproducible and organic solvent-free synthesis procedures and finely tunable mechanical features turn hydrogels into ideal candidates for use as biomaterials in drug delivery applications [3,4].

Polyelectrolytes (PE) in the form of ionic hydrophilic polymers have been widely used in pharmaceutical systems. Significant progress has been achieved in the development of new pharmaceutical technology platforms, based on ionic condensation between anionic or cationic PE with an ionizable drug (D) of opposite charge [5]. The acid-base interaction between the PE and the acidic or basic D is a valuable approach to yield new materials with physicochemical, pharmaceutical and biopharmaceutical properties different from those of their precursors. Ionic PE-D complexes can be obtained in a wide variety of qualitative

* Corresponding author at: Unitefa-Conicet, Departamento de Farmacia, Facultad de Ciencias Químicas, Universidad Nacional de Córdoba, Haya de la Torre esq. Medina Allende, Edificio de Ciencias II Ciudad Universitaria, X5000HUA Córdoba, Argentina.
E-mail address: alvaro@fcq.unc.edu.ar (A.F. Jimenez-Kairuz).

http://dx.doi.org/10.1016/j.msec.2016.06.071
0928-4931/

and quantitative compositions such as aqueous dispersions, gels or in the solid state. Eq. (1) shows the schematic representation of the acid-base interaction of an anionic PE and a basic drug, where *P-COOH* represents an acid PE, *D* is a basic drug, $P\text{-}COO^-$ is an ionized PE, DH^+ represents a protonated basic drug and $P\text{-}COO^-DH^+$ represents an ionic pair.

$$P\text{-}COOH + D \rightleftarrows P\text{-}COO^- + DH^+ \rightleftarrows \left[P\text{-}COO^-DH^+\right] \quad (1)$$

Previous reports proved that high proportions of *D* form ionic pairs with an oppositely charged PE, acting as a reservoir of D. According to the properties of the newly formed chemical entity, PE-D complexes can improve some unfavorable physicochemical or biopharmaceutical properties of recognized as safe and effective drugs such as low chemical stability in solution [6–8], low apparent solubility in the vehicle [9,10], low permeability through biological membranes [11,12], intracellular targeting [13], bacterial uptake [14], or modulation of drug release [15–17]. Therefore, these products are useful for the development of new drug delivery systems (DDS) [5,13,18–20].

Drug delivery technologies are always in need of new carrier materials with innovative properties that can enhance or improve control over the release profiles of any active pharmaceutical ingredient. Hence, stimuli-sensitive hydrogels (also known as smart hydrogels) are currently viewed as the new generation of carriers for biomedical applications [21–25].

In addition, the design of hydrogels based on highly functionalized or dendronized polymers is considered a novel alternative to smart carriers for controlled drug release due to their multivalent properties [26]. The development of hydrogels based on dendronized polymers that have acid groups is of particular interest to the pharmaceutical field. The acid functionality offers improved bioadhesion properties and confers the capacity to easily incorporate active pharmaceutical ingredients such as drugs, dyes and peptides into the hydrogel structures through ionic interaction or hydrolysable chemical bonds. Besides, the presence of acid groups offers the possibility of changing the macroscopic volume of their network structure with a change in pH [26].

Behera's amine (BA) is a commercially available dendritic amine developed by Raijani Behera of Newkome's research group [27]. The preparation of hydrogels based on this BA-derivative dendritic monomer (DM) was performed in our labs [26]. In a first step, the dendritic monomer (DM) was synthesized by reaction of amidation between Behera's amine (BA) and acryloyl chloride. Then, the *tert*-butyl ester groups were hydrolyzed with formic acid to yield the tri-acidic dendritic monomer, DM. Posterior, the synthesis of the hydrogels was performed from DM and the crosslinking agent, *N*,*N*-diallyltartardiamide (DAT). The chemical characterization, swelling behavior, rheology, fibroblast cytotoxicity and ionic drug load-release capacity of the new materials were studied in order to analyze the properties and the possibilities of biomedical application in drug delivery formulations. The influence of the pH environment on the swelling properties of the dendronized hydrogels was studied. It was clearly shown that the pH of the medium has considerable importance in the swelling properties of these ionic gels since %ESR is different depending on pHs. As example, in the case of one of the yielded hydrogels (HG 1.00/2) [26], the swelling capacity increases 6.3 times between pH 3 and 7. At pH 3, lower than pKa of the monomer, the carboxylic groups of the material are protonated. However, at pH 5 or 7, the acid groups are partially or totally deprotonated; consequently, the swelling is greater than at pH 3 because the electrostatic repulsion between the chains increases the water absorption capacity [26]. There are few reports on this subject.

Ciprofloxacin (CIP) is a fluoroquinolone antimicrobial agent with broad-spectrum antibacterial activity that is approved for the treatment of several infections by both, oral and topical administration [28]. In particular, topical pharmaceutical products, containing CIP between 0.2 and 0.3% w/w, are available as aqueous solutions, ointments or hydrogel forms. In aqueous solution, CIP exists mainly in their zwitterionic form owing to the acid/base interaction between the basic nitrogen of the piperazine and the carboxylic acid group. Such interaction also determines the low aqueous solubility of CIP at pH close to 7 [29].

In this context, the aim of this work was to explore the use of a dendronized polymer (DP) as a CIP carrier prepared under gel form, and to evaluate the physicochemical and *in vitro* drug release from DP-CIP complexes. Furthermore, the evaluation of biocompatibility and antimicrobial activity was conducted in order to define the potential use of these systems in the design of topical DDS.

2. Materials and methods

2.1. Materials

The following chemicals were used as purchased: ammonium persulfate (APS, Aldrich), tetramethylethylenediamine (TEMED, Aldrich) and (+)-*N*,*N*′-diallyltartramide (DAT, Aldrich), KH_2PO_4 p.a. (Anedra®, Bs.As., Arg.), NaCl p.a. (Parafarm®, Bs.As., Arg.), 1 N NaOH and HCl solutions (Anedra®, Bs.As., Arg.), and Carbopol® 934NF and 974P polymers (Lubrizol Adv. Mat. Inc., OH). The dendritic monomer (DM) BA-derivative, di-*tert*-butyl-4-acryloylamine-4-(2-*tert*-butoxycarbonylethyl) heptanoate, was synthesized according to a previous report [30]. Ciprofloxacin (CIP) free base was obtained by neutralization of CIP hydrochloride salt (Parafarm®, USP grade, Bs.As., Arg.) with 1.0 N NaOH solution, after which the precipitate was washed, filtered and dried at 100 °C until a constant weight was achieved.

2.2. Preparation and characterization of dendronized polymers

The general procedure for the synthesis of DP was previously reported by Cuggino et al. [26] and is represented in Fig. 1. The principal experimental descriptors of the DP^X synthesized for this work are reported in Table 1. Regarding the nomenclature of DP^X, the superscript "X" indicates that the hydrogel was prepared using an appropriate amount of DAT in relation to the total dendritic monomer (DM), expressed as mol%. For this particular work, DP containing 0.5, 2.0 or 4.0% crosslinking agent was synthesized following the general procedure. Thus, appropriate amounts of DM (1.0 M), DAT (0.5, 2.0 or 4.0 mol% with respect to DM) and APS (2 mol% with respect to DM) were dissolved in distilled water (4 mL), using a glass tube with a septum. This solution was then bubbled using N_2 for 2 min, and an appropriate volume of 0.32 M TEMED aqueous solution was added (2 mol% with respect to DM). Immediately, this solution mixture was transferred to a 5 mL disposable polypropylene syringe, which served as a reactor. The closed syringe was placed in a water bath at 25 °C for 24 h. After the reaction, the tips of syringe was carefully cut, the rigid rod-shaped form semisolid product was retired from the syringe barrel and then regular discs of about 3–4 mm thickness (about 1 cm in diameter) were cut. The discs were exhaustively washed in 500 mL of distilled water for 48 h (the solvent was changed every 12 h) to remove all of the unreacted monomer and then dried at 25 °C until a constant weight was achieved. The synthetic yield was calculated by gravimetry after polymer purification (Table 1), considering the percent of polymer mass recovery (%PMR) with respect to that of the mass of initial reagents (monomer and crosslinker). Finally, the dry discs were pulverized for the next studies.

For ^1H NMR characterization, approximately 5 mg of fine polymer powder was swelled in 0.8 mL of D_2O for 24 h before each measurement in order to facilitate water incorporation.

The swelling behavior of the DP^X products was determined by a gravimetric method. Approximately 35 mg of fine powder DP^X was weighed (m_d) in a pre-weighed tube. Then, 1.0 mL of ultrapure water was added to achieve swelling equilibrium at 25 °C for 24 h. The excess water was removed using a graduated pipette and the hydrogels inside the tubes were weighed (m_e). The percentage of

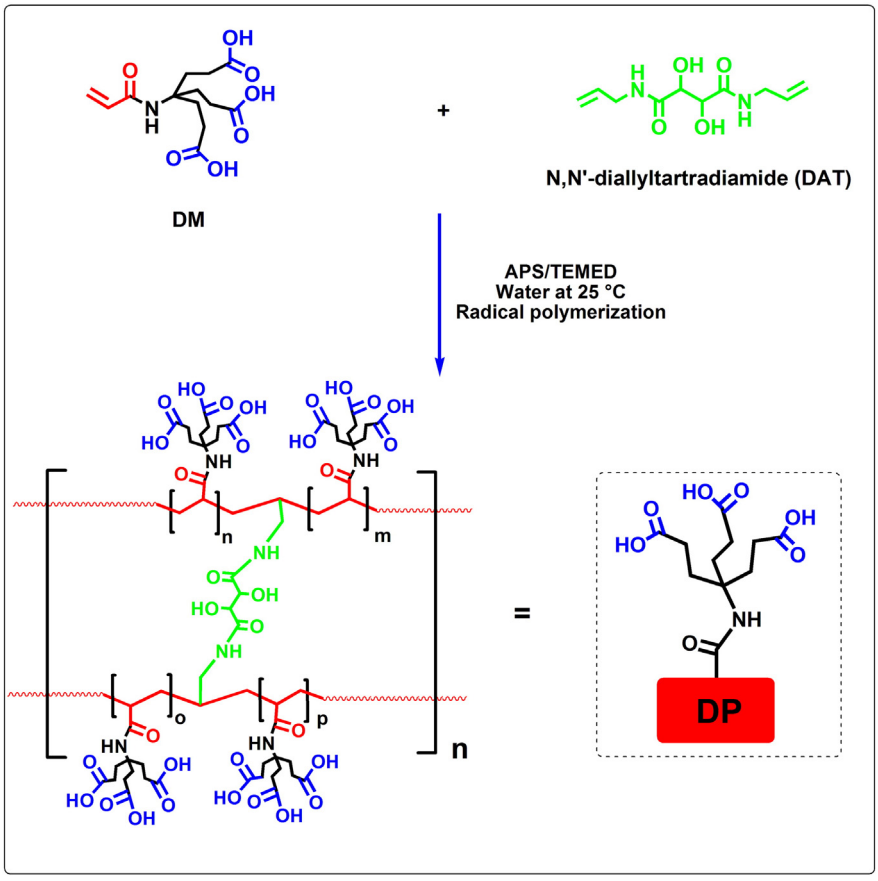

Fig. 1. Reaction scheme for the generation of dendronized polymers (DP) by free radical polymerization. Reagents and conditions: APS/TEMED; distilled water; 25 °C and 24 h (70–75% yield).

the swelling ratio at equilibrium (%ESR) was calculated according to Eq. (2).

$$\%\mathrm{ESR} = \left(\frac{m_e - m_d}{m_d}\right) \times 100 \quad (2)$$

2.3. Cytotoxicity studies of DP

A preliminary cytotoxicity screening was performed using XTT assay and Trypan blue dye exclusion on isolated human leukocytes from peripheral blood. Neutrophils and monocytes were isolated by a combined dextran/Ficoll-Hypaque sedimentation procedure. Sedimentation in dextran (6% solution) was performed before gradient centrifugation. A mixture of Ficoll-Hypaque (Histopaque-1077) was then used to isolate the mononuclear cells from the remaining haematic cells. The neutrophil layer was washed twice and suspended in Hanks' balanced salt solution (HBSS). Cell preparations were adjusted to 106 cells/mL for the assay. The viability of cells was estimated by Trypan blue dye exclusion [31] and XTT assay after 24 h of incubation at 37 °C with HBSS containing 2.5; 5 and 10 μL of control (Carbopol® 974P) and DP 0.5, 2 and 4% swollen at a proportion of 90 mg of sample to 4 mL of fresh culture medium. For XTT assay, 50 μL of the salt (1 mg/mL) was used. Three replicates for each exposure concentration were examined. Absorbance values at 450 nm were measured using a microplate spectrophotometer (Bio-Rad) [32]. All products showed viability around 70% in both assays which are available in Supporting information (Figs. S2 and S3).

In order to evaluate the cytotoxicity of DP on a monolayer of primary fibroblast cell line from human skin biopsy, DP^2 (DP containing 2% of crosslinker agent) was selected. This assay was carried out by direct contact of the swollen DP^2, at identical proportion of samples in fresh culture medium at 37 °C for 24 h with fibroblast cells, according to ISO standards [33]. Briefly, fibroblast cells were subcultured from a stock culture by trypsinization and seeded onto multi-well tissue culture plates. Cells were fed with Dulbecco's minimum essential medium supplemented with bovine serum and incubated at 37 °C in a 5% carbon dioxide atmosphere. When the cells attained a monolayer, 2.5, 5, and 10 μL of hydrogel swollen in fresh culture media (previously sterilized for 30 min by UV exposure) was carefully kept in contact with the cells for the direct contact assay in triplicate, with the aim of covering only one tenth of the cell surface. After incubation of the hydrogels in contact with the fibroblast cells for 24 h at 37 °C, their cytotoxicity was quantitatively determined by the MTT assay [34]. The cytotoxicity effect of the DP^2 was compared with that of the culture medium (used

Table 1
Composition and experimental parameters determined for the dendronized polymers.

DP^{X} [a]	DM (M)	DAT (%)	%PMR [b] (%)	%ESR [c] (%)
$DP^{0.5}$	1.0	0.5	70	6500
DP^{2}	1.0	2	75	2000
DP^{4}	1.0	4	73	1300

[a] A 2% molar ratio of ammonium persulfate (APS) and TEMED was used with respect to the DM for the preparation of all hydrogels.
[b] %PMR corresponds to polymer mass recovery determined from the dry weight of the final synthesis product with respect to the weight of monomers.
[c] %ESR is the percent swelling ratio, determined in water with the hydrogel powder at 25 °C.

as a control) and with two aqueous dispersions based on commercial anionic polymers frequently used in pharmaceutical and cosmetic formulations, Carbopol® 934NF and 974P, at similar concentrations.

2.4. Preparation of polyelectrolyte-drug complexes and physical mixtures

A dried disc of DP^X (where X = 0.5, 2.0 and 4.0) was crushed into a small particle powder using a mortar. Powder with a particle size of 117–140 μm was selected using analytical sieves. Series of complexes (DP^X–CIP_{25}) were prepared by adding an appropriate amount of CIP to neutralize 25% of the carboxylic groups of DP^X in the presence of 5 mL of ethanol per gram of polymer, considering that DP^X contains about 9.93×10^{-3} carboxylic group equivalents per 1.0 g of powdered material (theoretically estimated from the molecular weight of the monomers). Each mixture was gently stirred for 10 min and left to react at room temperature for 24 h. The products were dried at 40 °C until a constant weight was achieved. The physical mixtures (PM) were prepared in a mortar by smoothly mixing DP^X and CIP powders, in the same proportions used to prepare the complexes.

2.5. Physical and chemical characterization of complexes in solid state

2.5.1. Fourier Transform Infrared Spectroscopy (FTIR)

FTIR spectra (Avatar 360, ESP-Nicolet® Instrument Corp.) were measured from potassium bromide discs containing the sample (KBr, spectroscopy grade, Merck®). The discs were dried under vacuum for at least 2 h before recording the spectra. The samples were measured from 4000 to 400 cm^{-1} with a resolution of 8.0 cm^{-1} and 40 scans. Data were analyzed using specific software (OMNIC 5.1a Version, Nicolet Instrument Corp.).

2.5.2. Thermal analysis

DSC curves were obtained in a TA-Instruments MDSC-2920 cell using non-hermetic aluminum pans (pin hole) with about 1.1 ± 0.2 mg of sample, under a dynamic N_2 atmosphere (flow rate of 50 mL·min^{-1}) and a heating rate of 10 °C·min^{-1} in a temperature range of 25 to 300 °C. A first segment of heating between 25 and 120 °C, at 10 °C·min^{-1} with isothermal of 1 min, to dehydrated the samples was performed. The DSC cell was calibrated with *indium* (*m.p.* = 156.6 °C; $\Delta H_{fus} = 28.54\ J \cdot g^{-1}$). TG curves were obtained with a TA-Instruments Hi-Res-TGA 2950 thermobalance in a temperature range of 25 to 300 °C, using aluminum pans with approximately 2 mg of sample, under a dynamic N_2 atmosphere (50 mL·min^{-1}) and at a heating rate of 10 °C·min^{-1}. DSC and TG analyses were performed on samples of complexes, PM and pure CIP and DP^X.

2.5.3. X-ray powder diffraction (XRPD)

XRPD was used to identify crystalline phases and to qualitatively examine changes in the crystallinity of powdered materials. XRPD patterns were taken at room temperature in an X-ray diffractometer (PANalytical X'Pert Pro, NL.) in Bragg-Brentano geometry with Cu Kα radiation (λ = 1.5418 Å), a tube voltage of 40 kV and a current tube of 40 mA. The samples were placed in aluminum sample holders and the data were acquired over an angular range of 5 to 75° 2θ/θ, with a step of 0.02° 2θ/min.

2.5.4. Optical microscopy

The particle surface morphology was analyzed under an optical microscope with polarizing filters (Olympus® BX41, Olympus Corp., Japan), connected to a digital camera (Infinity 1, Lumera® Corp.) for image acquisition. The samples were processed with specific software (Infinity® Analyze, Release 5.0.2). Images were obtained with a magnification of 20×.

2.6. Preparation of gels based on PE-D complexes

Three series of gels were prepared from (DP^X-CIP_{25}) complexes (where "X" = 0.5, 2.0 and 4.0) using the following methodology: dry complexes (DP^X-CIP_{25}) were hydrated with a small amount of water (approximately 20% of the amount needed to yield dispersions of CIP at 1.0% w/v) by gently mixing in a mortar (a vigorous mixing can lead to an unwanted hydrophobic solid). Subsequently, a sufficient quantity of 1 N NaOH solution was added to neutralize 20% of the carboxylic groups of DP^X to yield (DP^X-CIP_{25})-Na_{20} semisolid dispersions. Finally, the remaining water was added in small aliquots, with continuous mixing to obtain physically stable, consistent and homogeneous dispersions, with a pale yellow color.

2.7. Characterization of gels based on PE-D complexes

2.7.1. pH measurement

The pH of the gel samples was determined with a pH-meter (SevenMulti, Mettler-Toledo, Sweden) equipped with a general-use combined glass electrode (InLab DG115-SC, Mettler-Toledo) at room temperature.

2.7.2. Ionic displacement by neutral salt titrations

The effect of the addition of sodium chloride on the ionic equilibrium of gels was evaluated through the titration of 20 mL of (DP^2-CIP_{25})-Na_{20} with a 0.9% NaCl solution. The pH of the dispersions was plotted against the proportion of NaCl added, expressed as mole % of neutral salt with respect to the total carboxylic groups of DP^X in the complex.

2.7.3. Rheological analysis

The rheological characterization of the gels was carried out using an Anton Paar® Physica MCR 301 rheometer. A 25 mm plate-plate (PP25) geometry and 1.0 mm gap was used for all of the experiments. An amplitude sweep (strain 0.01–20.0% at a constant angular frequency of 1 Hz) was performed on each prepared formulation at 37 °C to determine the storage moduli (G′), the loss moduli (G″), the linear viscoelastic region profiles (LVR) and the critical strain region of each product. A frequency sweep from 0.1 to 100 Hz at the maximum strain into LVR measured for each product (0.3–0.7% depending on each DP^X) was also performed at 37 °C to determine the performance of the material at different frequencies. In order to study the effect of CIP on the rheological properties of the systems, we analyzed gels of (DP^X-CIP_{25})-Na_{20} complexes and DP^X without CIP, both at a 1.2% polymer concentration (w/v).

2.7.4. Drug release studies

Drug release from (DP^X-CIP_{25})-Na_{20} semisolid dispersions was performed in a bicompartmental diffusion device (Franz cells) mounted with a semisynthetic cellulose membrane (12 kDa, Sigma-Aldrich, St. Louis, MO, USA). The effective diffusion area was 1.25 cm^2. The donor compartment was filled with a precisely weighed amount of each dispersion sample, close to 0.5 g, and kept in contact with 15 mL of receptor medium at 37 °C. Water, 0.9% NaCl and KH_2PO_4 0.2 M/NaOH 0.2 M USP buffer solution, pH 6.8, were used as receptor media. Samples of 1.0 mL of receptor medium were withdrawn at predetermined time intervals and replaced with equal quantities of fresh medium. The concentration of released drug was assayed spectrophotometrically at 272 nm (Evolution 300 BB, Termo-Sci Corp., USA). All experiments were carried out in triplicate and sink conditions were maintained. Release data were processed using the diffusion equation (Eq. (3)) proposed by Higuchi for semi-solid topical formulations [35].

$$M_t / M_\infty = k * t^{0.5} \quad (3)$$

where "M_t" is the amount of drug permeated at time "t", "M_∞" is the initial amount of drug in the donor compartment and "k" is the kinetic

Table 2
Kinetic data obtained from CIP release profiles processed by the Higuchi diffusion model.

Receptor medium	Amount of cross-linker (DAT)								
	0.5%			2.0%			4.0%		
	k^a	a	R^2	k^a	a	R^2	k^a	a	R^2
Water	1.36	−1.41	0.995	1.95	−1.32	0.987	2.20	−1.82	0.993
0.9% NaCl	12.02	−10.85	0.999	8.47	−8.27	0.994	7.25	−3.36	0.996
Buffer pH 6.8	1.85	−1.34	0.990	2.00	0.06	0.994	2.63	−0.57	0.992

[a] k is expressed in % $h^{-0.5}$.

constant. From linear analysis of the release profiles, plotting % of CIP release with respect to the square root of time, we calculated k, intercept values (a) and determination coefficients (R^2). R^2 was used to compare the fit of the profiles using this kinetic model (Table 2).

In addition, the release profiles were statistically compared using the similarity factor (f_2, Eq. (4)). Two profiles were considered similar when the f_2 value calculated between them was equal to or >50 [36].

$$f_2 = 50 \cdot \log\left\{\left(1 + \left(\frac{1}{n}\right)\sum_{t=1}^{n}(R_t - P_t)^2\right)^{-0.5} \cdot 100\right\} \quad (4)$$

2.7.5. Bacterial growth inhibition assay

A microbiological assay adapted from the method described in the Argentinean and US Pharmacopoeias [37–38] that applies the cylinder-plate diffusion technique, was used to analyze (DP^2-CIP_{25})-Na_{20} complexes, as gel form. The potencies of (DP^2-CIP_{25})-Na_{20} were evaluated in a comparative assay using CIP-free solution as a reference against *Pseudomonas aeruginosa* (ATCC 27853) and *Staphylococcus aureus* (ATCC 25923). The bioassay followed the 3 × 3 parallel line assay design (three doses of the reference and three of the sample in each plate), with six plates for each assay. In each plate, six stainless steel cylinders of the same size (8 × 6 × 10 mm) were placed on the surface of Müeller-Hinton agar inoculated with 1 mL of an overnight culture suspended in 0.9% NaCl sterile solution and adjusted to achieve a suspension turbidity of 25 ± 2% (transmittance) using a spectrophotometer set at 580 nm.

Three alternating cylinders were filled with 100 μL of the reference solutions (16, 32 and 64 μg/mL), and the other three cylinders were filled with sample solutions. The plates were incubated at 37 ± 1 °C aerobically for 18–24 h, the cylinders were removed and the diameters (mm) of the growth inhibition zone were carefully measured with a caliper. An analysis of variance (ANOVA) was used for statistical validation of the bioassays, by evaluating the regression, parallelism and linearity of each assay. The relative potency of (DP^2-CIP)$_{25}$-Na_{20} was calculated according to the Argentinean Pharmacopoeia [37]. Furthermore, the effect of drug-free polymer was also assessed by this methodology.

2.7.6. Acute skin irritation test

Acute skin irritation of DP^2-Na_{20} and (DP^2-CIP_{25})-Na_{20} was evaluated on rabbits using the Draize score test [39]. This test was performed according to the guidelines established by Resolution 288/90 from the Ministry of Health of Argentina and Standard ISO [33,40], using an experimental protocol approved by the Ethical Committee for Rational Use of Experimentation Animals (Facultad de Ciencias Químicas, Res. No. 402/2014, 04/09/2014). Six New Zealand albino rabbits weighing 2.5–3.5 kg were used. The animals were provided with food and water *ad libitum* in a temperature-controlled room (21 ± 5 °C) and exposed to light-dark cycles of 12 h. Twenty-four hours prior to beginning the study, an area on the back of rabbits was shaved (8 × 8 cm) and then washed with purified water. Each rabbit was treated with 0.5 mL of DP^2-Na_{20} and (DP^2-CIP_{25})-Na_{20}, applied over a 16 cm^2 area of hair-free skin. The skin was observed for erythema or edema at 24, 48 and 72 h after application, and assigned values between 0 and 4 according to the Draize score. In addition, distilled water was used as a negative control and a 20% w/v sodium dodecyl sulfate (SDS) solution was used as a positive control for both edema and erythema.

3. Results and discussion

3.1. Synthesis and characterization of dendronized polymers

Fig. 1 shows the scheme for the preparation of DP^X by free radical polymerization in aqueous solution, using DM as the monomer, DAT as the cross-linking agent, and APS/TEMED as the initiator and activator of the generation of free radicals, respectively [21]. All DP^X products were obtained in rod-shaped form, cut in disc, washed, dried and then powdered for future studies. Table 1 includes their experimental descriptors. After elimination of DM and DAT traces by aqueous washing, a high production yield of DP^X was obtained that showed a polymer mass recovery (%PMR) between 70 and 75%. After purification, the completion of the DM polymerization reaction was studied by ^{1}H NMR as the disappearance of its characteristic vinyl bands between δ: 5.70 and 6.29 ppm on the spectra of the dendronized polymers (Fig. S1, Supporting information). The effect of the variation in the proportion of DAT on the DP^X swelling capacity was studied. As expected, the increase in the amount of crosslinking agent led to a proportional decrease in the water swelling capacity (%ESR) of DP^X (see Table 1).

3.2. Cytotoxicity studies

Fig. 2 shows the effects of dispersions prepared from DP^2 and other commercial polymers on the cell viability of fibroblast cells. Interestingly, the new DP-based hydrogels showed cell viability above 70% at all concentrations assayed. In addition, identical results would be yielded with DP^X containing 0.5 and 4% of cross-linking agent, according with preliminary viability assays realized using isolated human leukocytes from peripheral blood (Figs. S2 and S3, Supporting information). These levels of cell viability were similar to or higher than that exhibited by the Carbopol® 934NF and 974P-based hydrogels. It is important to emphasize that the Carbopol® polymers are generally regarded as essentially nontoxic and nonirritant materials and widely used in pharmaceutical products. There is no evidence in human of hypersensitivity reactions to Carbopol® used topically [41].

In vitro cytotoxicity studies provide a valuable preliminary evaluation of synthetic polymers and other materials that are frequently used to define biomaterials. According to ISO 10993-5 standards [33], DP^2 would be considered a non-toxic material, providing considerable improvement over current products for topical biomedical applications.

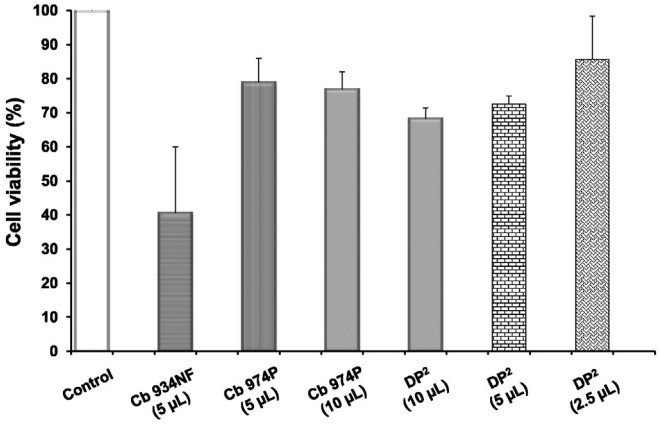

Fig. 2. Viability of fibroblast cells incubated with pure culture medium (control) and dispersions of Carbopol® (Cb) 934NF, 974P and DP^2 swollen at different concentrations.

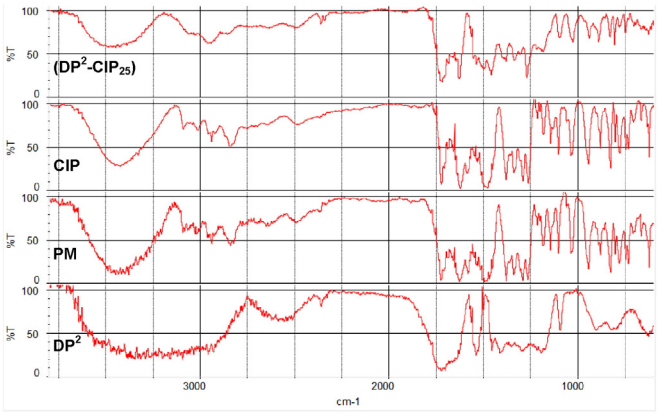

Fig. 3. FTIR spectra of the (DP^2-CIP_{25}) complex, CIP, DP^2 and the physical mixture.

3.3. Characterization of ionic complexes in the solid state

Complexes of (DP^X-CIP_{25}) in the solid state were characterized through FTIR, thermal analysis, XRPD and optical microscopy, and compared with pure materials and the physical mixture (PM).

Fig. 3 shows the FTIR spectra obtained from (DP^2-CIP_{25}), the precursors and the PM. The changes in the spectra, arising from the acid-base interaction between DP and CIP, were evaluated.

The spectra corresponding to the complex and to the PM were quite similar. Nevertheless, it was possible to analyze changes through a deconvolution process. Hence, signals at 1333 and 1557 cm^{-1} observed in the deconvolution of the spectrum and corresponding to the (DP^2-CIP_{25}) complex were attributed to vibrations, due to symmetric and asymmetric stretch of the carboxylate group [42–44]. In addition, a broad band at 2500 cm^{-1}, attributed to the protonation of the piperazinyl-ring N atom (NH_2^+), was observed [19,44]. These results demonstrate that CIP could be predominantly ionically-bonded to DP carboxylic pendant groups. For more detailed analysis, FTIR and deconvolution spectra from 2000 to 1000 cm^{-1} are available in Supporting information (Figs. S4 and S5, Supporting information).

Fig. 4 shows the comparative thermal analysis by DSC and TG. Thermograms of the (DP^2-CIP_{25}) complex are shown as representative of thermal behavior of the (DP^X-CIP_{25}) products yielded. For the (DP^2-CIP_{25}) complex, the melting endotherm peak of CIP, at 271–272 °C, was not present. However, a minimal endothermic process was observed below the melting temperature of CIP (around 258 °C) and substantially lower than would be expected for the amount of CIP in the sample indicating the absence of free drug or crystalline complex in the solid state. Likewise, TG curves showed the loss of two masses. The first, around 100 °C, could be assigned to a loss in humidity; the other, at 273 °C, to CIP decomposition. On the other hand, the analysis of the PM showed a thermal profile similar to that of the complex, showing an endothermic process at about 265 °C. This behavior could be related to a drug-polyelectrolyte reaction in the solid state, probably favored by heating, resulting in a solid phase transition from the crystalline to the amorphous form of CIP in the presence of DP.

Fig. 5 depicts the representative XRPD patterns of all powder materials. The pattern of the (DP^2-CIP_{25}) complex clearly shows a characteristic profile of an amorphous compound; no typical reflections of crystalline CIP are present. However, the PM pattern shows the characteristic peaks of CIP, denoting the crystalline character of CIP and the absence of an interaction with DP. The disappearance of the CIP peaks in the complexes suggests the absence of free drug, in addition to a complete interaction between CIP and DP^2.

Representative optical microscopy images of the (DP^2-CIP_{25}) complex, DP^2, CIP and their PMs, with and without polarized light, were obtained as shown in Fig. 6. In line with the XRPD results, the (DP^2-CIP_{25}) complex could only be observed without polarized light, since the reaction between CIP and DP gave an amorphous solid and did not present the phenomenon of birefringence [45]. On the other hand, under polarized light, the PM showed the phenomenon of birefringence, ascribed to small crystals of CIP that had not reacted with DP. The pure CIP showed behavior similar to that of the PM, which is typical for anisotropic solid materials (Fig. 6).

3.4. Characterization of gels based on (DP^X-CIP_{25})-Na_{20} complexes

The (DP^X-CIP_{25})-Na_{20} complex-based gels appeared as opaque and viscous dispersions that were pale-yellow in color (Fig. 7). The pH of the series was in the range of 6.2 to 6.8, which is considered optimal for topical application to mucosal membranes or skin lesions [46].

Fig. 8a shows that the LVR for (DP^X-CIP_{25})-Na_{20} semisolid dispersion prepared using $DP^{0.5}$, DP^2 and DP^4 was between 0.01–10, 0.01–1.20 and 0.01–1.00%, respectively. Thus, the G′ values of all materials decreased above the critical strain (CS) region, which proved slightly different according to the amount of crosslinker in each product, resulting in CS = 10% for ($DP^{0.5}$-CIP_{25})-Na_{20}; CS = 1.20% for (DP^2-CIP_{25})-Na_{20} and CS = 1% for (DP^4-CIP_{25})-Na_{20}. $DP^{0.5}$ alone (without CIP) did not show viscoelastic behavior as compared with the gels prepared with CIP. It was very difficult to determine the LVR for $DP^{0.5}$ because the viscous character prevailed over the viscoelastic one. The G′ was particularly low and depended upon the strain applied. The situation was different when CIP was loaded into DP^X, since the sample was gel-like and G′ increased considerably. Thus, the incorporation of CIP into the polymer conferred improved rheological characteristics in comparison with DP without

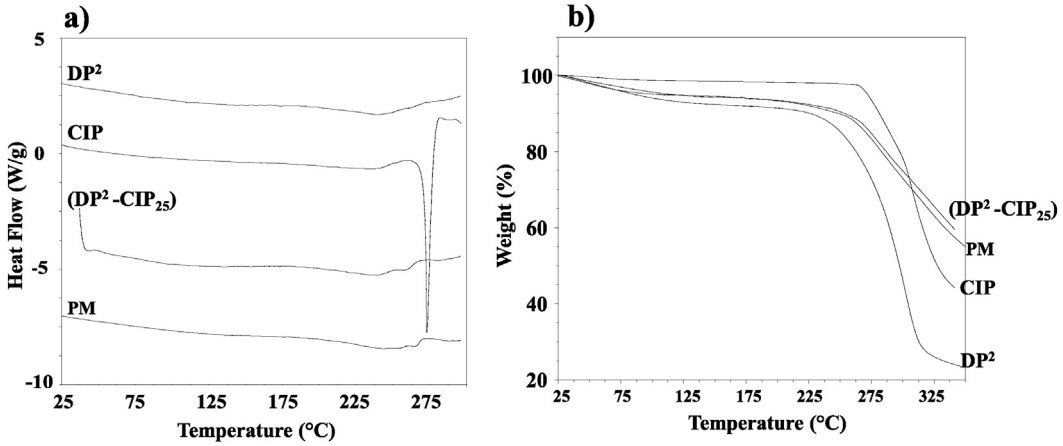

Fig. 4. (a) DSC and (b) TG curves for: the (DP^2-CIP_{25}) complex, DP^2, CIP and the physical mixture (PM).

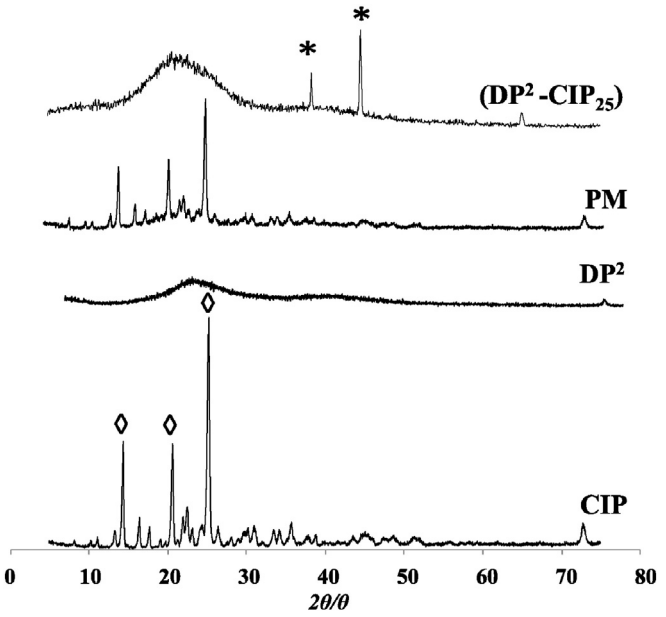

Fig. 5. XRPD patterns of DP^2, CIP, the (DP^2-CIP_{25}) complex and the PM. Peaks for pure CIP (◊) and the aluminum holder (*) are also indicated.

drug. The improvement of the mechanical properties of the (DP^X-CIP_{25})-Na_{20} complexes could be attributed to the strong ionic interaction between the amino groups of the drug and the acid groups of the dendritic polymer, which increased the hardness of the polymer network, as showed in Fig. 8.

After determination of the LVR of the products, the response over a range of frequencies was examined at constant strain within the LVR. G′ and G″ served as a function of angular frequency at the maximum strain into LVR obtained for each DP^X-CIP_{25}-Na_{20} complexes (between 0.3 and 0.7%). As seen in Fig. 8b, all of the (DP^X-CIP_{25})-Na_{20} complexes displayed a single plateau region in their dynamic modules. In addition, G′ values had good elastic responses and were, in all cases, larger than G″ values over the entire frequency range. The elastic behavior of the samples predominated over the viscous nature and all products exhibited mechanical rigidity. In addition, at increasing frequencies, *i.e.* at a low relaxation time, the flexibility decreased and the swollen samples became increasingly rigid. This behavior is generally found in polymers with slightly crosslinked networks. G′ and G″ values for the complexes were G′ = 72 Pa, G″ = 10 Pa; G′ = 525 Pa, G″ = 22 Pa; and G′ = 1330 Pa, G″ = 180 Pa for ($DP^{0.5}$-CIP_{25})-Na_{20}; (DP^2-CIP_{25})-Na_{20} and (DP^4-CIP_{25})-Na_{20}, respectively.

Interestingly enough, G′ and G″ for ($DP^{0.5}$-CIP_{25})-Na_{20} and (DP^2-CIP_{25})-Na_{20} were on the same order as those reported by Bonacucina et al. for Carbopol® 974P aqueous dispersions (Carbopol® 974P at 2% w/v G′ = 35 Pa and G″ = 7.4 Pa; Carbopol® at 4% w/v G′ = 360 Pa and G″ = 25 Pa) [47]. As shown, the G′ values of the gels depend on the amount of crosslinking agent in the structures. As expected, DP^4 yielded hydrogels with the greatest G′ values. The higher degree of crosslinking points in DP^X increased the solid component of the final structure. This result opens up the possibility of changing the mechanical properties of the complex by modifying the amount of crosslinking points in the polymers according to different requirements.

In addition, the rheological behaviors are in line with the swelling behavior of the hydrogels since the sample with the greater amount of crosslinker (DP^4) showed a lesser degree of swelling or, in rheological terms, a more elastic structure.

As a complement to their mechanical properties, all of the new complexes were able to flow through the syringes, as shown in Fig. 7, which means that the material flows when a deformation is applied. This thixotropic behavior of the hydrogels is a desirable property for the development of DDSs for topical applications [48].

3.5. Ionic exchange analysis

In order to show the ionic interaction between DP and CIP and CIP release by ionic displacement from the complex, titration of complex gels with a neutral salt was performed. Fig. 9 shows a progressive decrease of pH as an increasing amount of NaCl was added to the (DP^2-CIP_{25})-Na_{20} complex.

The addition of NaCl to the (DP^X-CIP_{25})-Na_{20} complex should produce drug displacement according to the equilibrium depicted in Eq. (5), causing a protogenic effect.

$$\left[P\text{-}COO^{-}H^{+}\text{-}CIP\right] + NaCl \rightleftarrows P\text{-}COO^{-}Na^{+} + CIP + H^{+} + Cl^{-} \tag{5}$$

Therefore, it is clear that the ionic exchange between Na^+ and the protonated species of CIP (H^+-*CIP*) produces the main contribution to the pH shift. The plot also showed that even after addition of

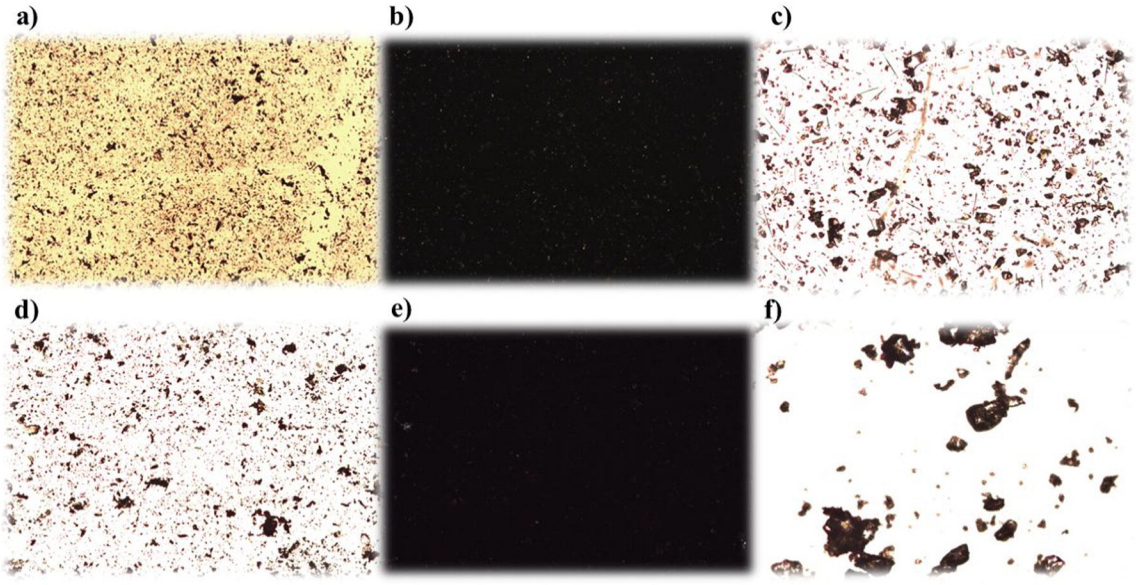

Fig. 6. Representative optical microscopy images corresponding to: a) CIP; b) CIP under polarized light; c) DP^2; d) PM; e) PM under polarized light; and f) (DP^2-CIP_{25}) complex.

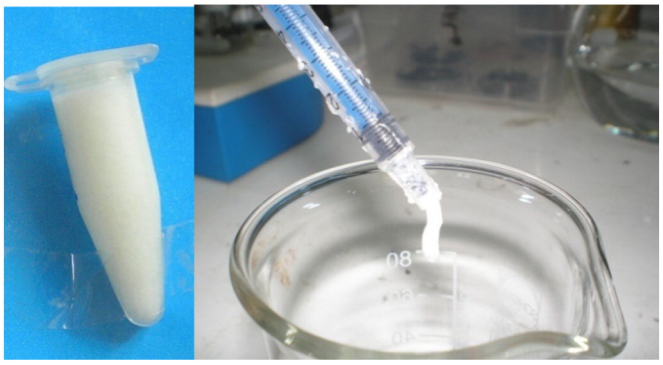

Fig. 7. Syringe extrusion of the gel based on the $(DP^{X}\text{-}CIP_{25})\text{-}Na_{20}$ complex.

300 mol% of NaCl, the pH decreases slowly, revealing the high stability of the complex toward ionic exchange with small ions.

3.6. In vitro drug release studies

CIP release behavior from $(DP^{X}\text{-}CIP_{25})\text{-}Na_{20}$ complexes was studied to evaluate the potential for a topical drug delivery application. Fig. 10 shows CIP release profiles from gels containing 1.0% CIP. Using water as the receptor medium, a very slow release of CIP from $(DP^{X}\text{-}CIP_{25})\text{-}Na_{20}$ gels was observed (Fig. 10a). The cumulative percent of total drug released after 24 h was <10% for the entire set, showing no significant differences ($f_2 = 85.8$) in relation to the amount of crosslinking agent in the gel.

On the other hand, when 0.9% NaCl was used as the receptor medium instead of distilled water, an increase in the drug release rate of 4 to 16 times was observed for $(DP^{2}\text{-}CIP_{25})\text{-}Na_{20}$ and $(DP^{0.5}\text{-}CIP_{25})\text{-}Na_{20}$, respectively. The release profiles of CIP from complexes with 2 or 4% crosslinking agent were very similar and showed no significant changes ($f_2 = 82.6$), as compared with greater increases in the amount of crosslinking agent. However, similarity factor applied to release profiles of $(DP^{2}\text{-}CIP_{25})\text{-}Na_{20}$ in water and saline solution showed $f_2 = 49.1$, denoting significant changes of CIP release.

In addition, release profiles fit well to a Higuchi model (Eq. (3)) and no significant differences were observed among the complexes with 2 or 4% crosslinking agent across the different receptor media (Table 2).

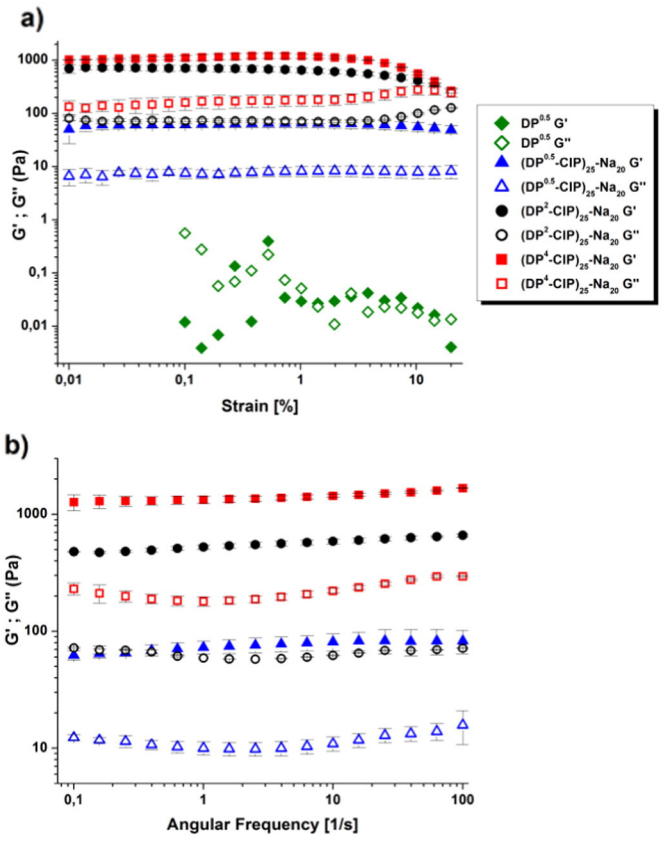

Fig. 8. a) Amplitude sweep assay for $DP^{0.5}$; $(DP^{0.5}\text{-}CIP)_{25}\text{-}Na_{20}$; $(DP^{2}\text{-}CIP)_{25}\text{-}Na_{20}$ and $(DP^{4}\text{-}CIP)_{25}\text{-}Na_{20}$ at 37 °C; b) frequency sweep for $(DP^{0.5}\text{-}CIP)_{25}\text{-}Na_{20}$; $(DP^{2}\text{-}CIP)_{25}\text{-}Na_{20}$ and $(DP^{2}\text{-}CIP)_{25}\text{-}Na_{20}$ at 37 °C.

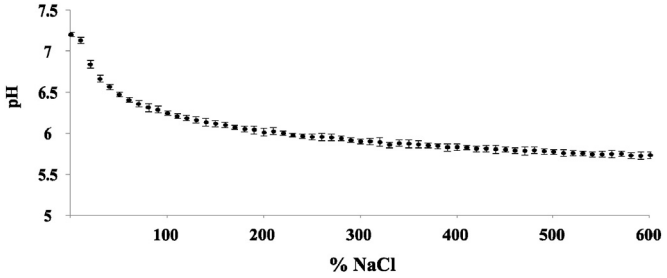

Fig. 9. pH changes in an aqueous dispersion of the $(DP^{2}\text{-}CIP)_{25}\text{-}Na_{20}$ complex due to displacement of CIP by ionic exchange with NaCl.

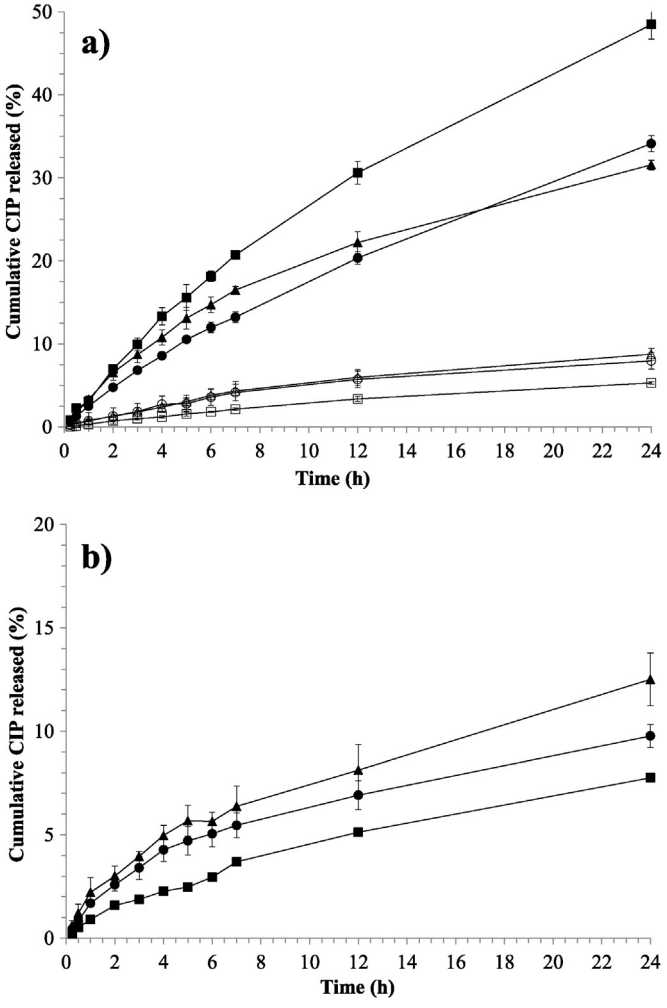

Fig. 10. *In vitro* CIP release profiles from $(DP^{X}\text{-}CIP)_{25}\text{-}Na_{20}$ using Franz cells filled with a) ultrapure water (empty symbols), 0.9% NaCl (filled symbols) and b) pH 6.8 buffer solutions as receptor media. Symbols: ■ $(DP^{0.5}\text{-}CIP)_{25}\text{-}Na_{20}$, ● $(DP^{2}\text{-}CIP)_{25}\text{-}Na_{20}$ and ▲ $(DP^{4}\text{-}CIP)_{25}\text{-}Na_{20}$.

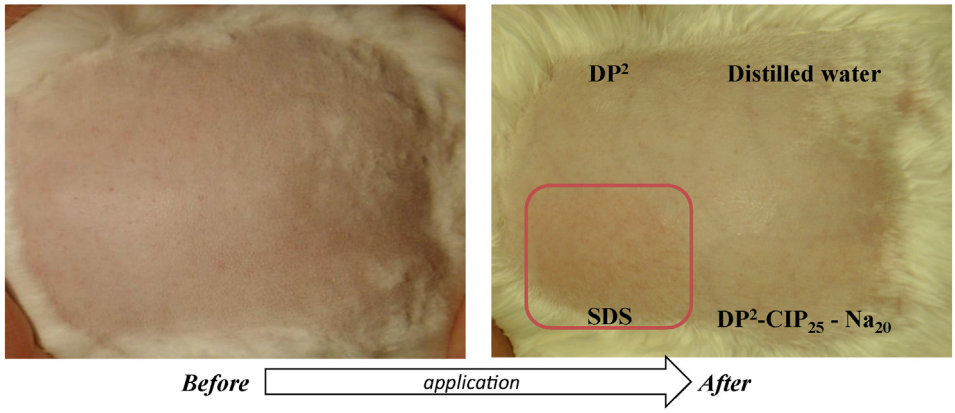

Fig. 11. Evaluation of acute dermal irritation for DP^2 and (DP^2-CIP_{25})-Na_{20}. Distilled water and sodium dodecyl sulfate (SDS) were used as negative and positive controls, respectively.

A model of the drug release mechanism from PE-D complexes was previously proposed [49,50]. Briefly, according to Eq. (1), release toward water as a receptor medium occurs essentially through Fickian diffusion of the neutral species *D* since diffusion of DH^+ is mainly prevented by the electrostatic gradient produced by the polyanion. Consequently, the diffusion rate of *D* is higher than that of DH^+. As *D* diffuses away from the complex environment, the equilibrium quickly responds to provide fresh, free *D*, acting as a CIP reservoir.

On the other hand, the presence of concentrated ions in the receptor medium has an important role in promoting ionic exchange. As described by Eqs. (1) and (5), the diffusion of Na^+ and Cl^- ions from the receptor to the gel compartment allows for free diffusion of charged CIP species attached to DP^X. In relation to this point, it should be noted that the saline composition of biological fluids would promote CIP release from polymeric carriers.

Release results are consistent with the view that a high proportion of CIP is present in the form of ionic pairs. Thus, if delivery occurs through the Fickian diffusion of free species and their concentrations are low by the high proportion of ionic pairs, then the delivery rate should remain slow, as observed when water was used as the receptor medium. In addition, this result suggests that the dissociation of ion pairs is the slow step that controls rate delivery. As Na^+ and Cl^- diffuse into the gel, Na^+ promotes the exchange of cationic and zwitterionic species of CIP attached to DP^X, while Cl^- acts as a counter ion to diffuse with them. Both mechanisms contribute to increase the CIP delivery rate.

Finally, CIP release from the gels toward phosphate buffer solution (pH 6.8) as a model of topical and mucosal physiological fluid was performed. As seen in Fig. 10b, an extended release of CIP from (DP^X-CIP_{25})-Na_{20} were observed. CIP was slowly released from the gelling dispersions by Fickian diffusion kinetics and no >12% of the CIP was delivered in 24 h. Although minimal differences can be observed between the release profiles with different proportion of the crosslinker agent, not significant differences between them were found, showing $f_2 = 78.8$ for ($DP^{0.5}$-CIP_{25})-Na_{20} and (DP^4-CIP_{25})-Na_{20} release profiles. So, they can be considered similar.

In addition, the comparative analysis of CIP release profiles using water and phosphate buffer solution results in similar behavior, showing $f_2 = 71.2$ for ($DP^{0.5}$-CIP_{25})-Na_{20} and (DP^4-CIP_{25})-Na_{20} in water and buffer solution, respectively. This result was also consistent with the low solubility of CIP in phosphate buffer solution at pH 6.8. This would be the determining step in the release control, despite the fact that the systems based on DP^X presented swelling values in pH 6.8 buffer solution higher than in water [26]. However, complementary studies could be useful to evaluate the exchange efficiency of phosphate and its interaction with the polymeric network.

3.7. Acute dermal irritation analysis

Fig. 11 shows a representative photograph of the back of rabbits after application of the complexes, pure DP^X and controls. The observational analysis of the skin surface of the rabbits over 72 h post-administration, showed total absence of edema and erythema for both products in all animals. According to Draize test scoring, both DP^2 and (DP^2-CIP_{25})-Na_{20} could be classified as "practically non-irritating" materials, showing a score < 0.99. These data, in combination with the results of the acute cytotoxicity studies, denote the high biocompatibility of the new products.

3.8. Bacterial growth inhibition results

The antibacterial activity of the (DP^2-CIP_{25})-Na_{20} ionic complex was investigated by measuring its ability to inhibit Gram-positive and Gram-

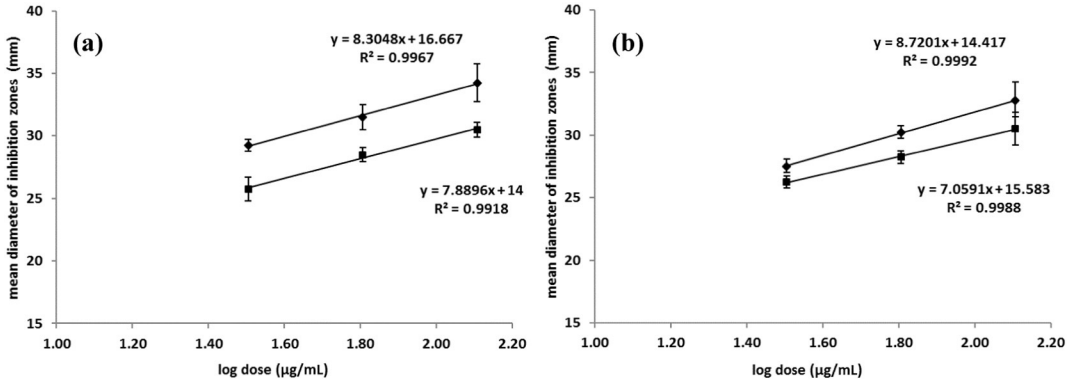

Fig. 12. Dose-response curves exhibited by DP^2-CIP_{25}-Na_{20} (■) and CIP (●) against (a) *S. aureus*, ATCC 25923 and (b) *P. aeruginosa*, ATCC 27853 obtained by the microbiological cylinder-plate assay.

negative bacterial growth, in comparison with an aqueous CIP solution. Antibiotic assays must be designed in such a way that allows the mathematical model's validity to be examined on the basis of a potency equation. According to the Argentinean [37] and US Pharmacopoeias [38], if a parallel-line model is chosen, the log dose–response line of the preparation to be examined, as well as the reference preparation, must be parallel and linear over the range of doses used in the determination. These conditions were verified by validity tests for a given probability by means of an ANOVA. No deviation from parallelism or linearity was found ($p > 0.05$), and the regression analysis was highly significant ($p < 0.05$).

The gel based on the ionic complex (DP^2-CIP_{25})-Na_{20} inhibited bacterial growth. However, (DP^2-CIP_{25})-Na_{20} showed a potency of 38 and 58% of that of the CIP hydrochloride solution at similar CIP concentrations, against *S. aureus* and *P. aeruginosa*, respectively (Fig. 12). These data suggest a slow CIP release from the ionic pairs in the gel. On the other hand, no inhibitory effect was found for the drug-free polymer.

In the bioassay, CIP diffuses into the agar and inhibits the growth of the organism. The diameter of the inhibition zone is proportional to the concentration of antibiotic in the sample. However, multiple variables affect the diameter of the inhibition zone. Taking into account the modulation of drug release by (DP^X-CIP_{25})-Na_{20} that was observed in the Franz cell experiments, the difference between the lowest antimicrobial potency exhibited by the sample under evaluation compared with that of free CIP could be attributed to the fact that the polymer-drug interaction delays drug diffusion from the cylinders. This lower concentration gradient around them leads to the formation of inhibition zones of smaller size. It is important to note that both *S. aureus* and *P. aeruginosa* are the main opportunistic pathogen microorganisms found in topical and mucosal infections [51,52].

Finally, *in vitro* tests revealed that the release of CIP from these gels was appropriate, both in terms of magnitude and velocity for the potential use of (DP^X-CIP_{25})-Na_{20} complexes for the design of topical antimicrobial controlled-release systems. It is expected that these gels, based on polyelectrolyte-drug complexes, would provide a slow and sustained release of CIP after topical administration, with the capacity to maintain a suitable concentration of CIP above the minimal inhibitory concentration, for long periods of time, without altering the biostructures of skin or mucous membranes.

4. Conclusions

New CIP controlled-release gels with the potential for topical administration were developed using a novel synthetic, non-toxic and biocompatible dendronized polymer. The loading of CIP, under ionic form, into the dendronized polymer network was easily achieved by attractive ionic interaction, as confirmed by numerous analytical techniques. Dispersions of (DP^X-CIP_{25})-Na_{20} yielded physically stable products with excellent mechanical behaviors. No skin irritation was observed, which is a key advantage for topical application. The complexes were able to constantly release CIP by ionic exchange, acting as a CIP reservoir. In addition, they showed acceptable antimicrobial potency. The products based on (DP^X-CIP_{25})-Na_{20} showed very promising properties that could be exploited for the treatment of topical and mucosal opportunistic infections.

Acknowledgments

The authors thank Secretaría de Ciencia y Tecnología, Universidad Nacional de Córdoba (SECyT-UNC, 2014-2015, N°: 30720130100922CB), Consejo Nacional de Investigaciones Científicas y Técnicas (CONICET, PIP 2013-2016, N°: 11220120100461) and at Ministerio de Ciencia, Tecnología e Innovación Productiva (FONCyT-program, PICT 2012-0173) for financial support and facilities. García MC, Cuggino JC and Rosset CI thank CONICET for doctoral and postdoctoral fellowships. A special thanks to Lubrizol Argentina for generously providing Carbopol® sample.

Appendix A. Supplementary data

Supplementary data to this article can be found online at http://dx.doi.org/10.1016/j.msec.2016.06.071.

References

[1] K.A. Pal, K. Banthia, D.K. Majumdar, Polymeric hydrogels: characterization and biomedical applications – a mini review, Designed Monomers and Polymers 12 (2009) 197–220.
[2] Y. Fu, W.J. Kao, Drug release kinetics and transport mechanism of non-degradable and degradable polymeric delivery systems, Expert Opin. Drug Deliv. 7 (2010) 429–433.
[3] J. Kopecek, Hydrogels: from soft contact lenses and implants to self assembled nanomaterials, J. Polym. Sci. A Polym. Chem. 47 (2009) 5929–5946.
[4] J.A. Johnson, N.J. Turro, J.T. Koberstein, J.E. Mark, Some hydrogels having novel molecular structures, Prog. Polym. Sci. 35 (2010) 332–337.
[5] S. De Robertis, M.C. Bonferoni, L. Elviri, G. Sandri, C. Caramella, R. Bettini, Advances in oral controlled drug delivery: the role of drug—polymer and interpolymer non-covalent interactions, Expert Opin. Drug Deliv. 12 (2014) 1–13.
[6] A.F. Jimenez-Kairuz, D.A. Allemandi, R.H. Manzo, The improvement of aqueous chemical stability of a model basic drug by ion pairing with acid groups of polyelectrolytes, Int. J. Pharm. 269 (2004) 149–156.
[7] S.L. Esteban, R.H. Manzo, F.L. Alovero, Azithromycin loaded on hydrogels of carbomer: chemical stability and delivery properties, Int. J. Pharm. 366 (2009) 53–57.
[8] A. Zoppi, Y. Garro Linck, G.A. Monti, D.B. Genovese, A.F. Jimenez-Kairuz, R.H. Manzo, M.R. Longhi, Studies of pilocarpine: carbomer intermolecular interactions, Int. J. Pharm. 427 (2) (2012) 252–259.
[9] M.S. Ardusso, R.H. Manzo, A.F. Jimenez-Kairuz, Comparative study of three structurally related acid polyelectrolytes as carriers of basic drugs: carbomer, Eudragit L-100 and S-100, Supramol. Chem. 22 (2010) 289–296.
[10] W.G. Dai, C.D. Liang, Y.Q. Song, Nanosizing of a drug/carrageenan complex to increase solubility and dissolution rate, Int. J. Pharm. 342 (2007) 201–207.
[11] M.V. Ramírez-Rigo, M.E. Olivera, M. Rubio, R.H. Manzo, Enhanced intestinal permeability and oral bioavailability of enalapril maleate upon complexation with the cationic polymethacrylate Eudragit E100, Eur. J. Pharm. Sci. 55 (2014) 1–11.
[12] M.C. Bonferoni, G. Sandri, S. Rossi, F. Ferrari, S. Gibin, C. Caramella, Chitosan citrate as multifunctional polymer for vaginal delivery. Evaluation of penetration, enhancement and peptidase inhibition properties, Eur. J. Pharm. Sci. 33 (2008) 166–176.
[13] F.D. Battistini, J. Flores-Martin, M.E. Olivera, S. Genti-Raimondi, R.H. Manzo, Hyaluronan as drug carrier. The *in vitro* efficacy and selectivity of hyaluronan-doxorubicin complexes to affect the viability of overexpressing CD44 receptor cells, Eur. J. Pharm. Sci. 65 (2014) 122–129.
[14] V.L. Romero, R.H. Manzo, F.L. Alovero, Enhanced bacterial uptake and bactericidal properties of ofloxacin loaded on bioadhesive hydrogels against *Pseudomonas aeruginosa*, J. Chemother. 22 (2010) 328–334.
[15] M.L. Guzmán, R.H. Manzo, M.E. Olivera, Eudragit E100 as a drug carrier: the remarkable affinity of phosphate ester for dimethylamine, Mol. Pharm. 9 (2012) 2424–2433.
[16] M.C. Palena, R.H. Manzo, A.F. Jimenez-Kairuz, Self-organized nanoparticles based on drug-interpolyelectrolyte complexes as drug carriers, J. Nanopart. Res. 14 (2012) 867–871.
[17] D.A. Quinteros, D.A. Allemandi, R.H. Manzo, Equilibrium and release properties of aqueous dispersions of non-steroidal anti-inflammatory drugs complexed with polyelectrolyte Eudragit E100, Sci. Pharm. 80 (2012) 487–496.
[18] F.D. Battistini, M.E. Olivera, R.H. Manzo, Equilibrium and release properties of hyaluronic acid–drug complexes, Eur. J. Pharm. Sci. 49 (2013) 588–594.
[19] J.M. Bermúdez, A.F. Jimenez-Kairuz, M.E. Olivera, D.A. Allemandi, R.H. Manzo, A ciprofloxacin extended release tablet based on swellable drug polyelectrolyte matrices, AAPS Pharm. Sci. Tech. 9 (2008) 924–930.
[20] M.C. Palena, M.S. Ardusso, R.H. Manzo, A.F. Jimenez-Kairuz, Polyelectrolytes as drug carriers. Analysis by dynamic light scattering of reconstituted and in-situ prepared model polymethacrylate-drug aqueous dispersions, Open Nanosci. J. 4 (2010) 1–7.
[21] E.A. Appel, J. del Barrio, X.J. Loh, O.A. Scherman, Supramolecular polymeric hydrogels, Chem. Soc. Rev. 41 (2012) 6195–6214.
[22] Q.Q. Dou, S.S. Liow, E. Ye, R. Lakshminarayanan, X.J. Loh, Biodegradable thermogelling polymers: working towards clinical applications, Adv. Healthcare Mater. 3 (2014) 977–988.
[23] S.S. Liow, Q. Dou, D. Kai, A.A. Karim, K. Zhang, F. Xu, X.J. Loh, Thermogels: In Situ Gelling Biomaterial, ACS Biomater. Sci. Eng. 2 (3) (2016) 295–316.
[24] A.S. Hoffman, Stimuli-responsive polymers: biomedical applications and challenges for clinical translation, Adv. D. Del. Rev. 65 (2013) 10–16.
[25] J.C. Cuggino, C.B. Contreras, A.F. Jimenez-Kairuz, B.A. Maletto, C.I. Alvarez Igarzabal, Novel poly(NIPA-co-AAc) functional hydrogels with potential application in drug controlled release, Mol. Pharm. 11 (7) (2014) 2239–2249.
[26] J.C. Cuggino, G. Charles, G. Gatti, M.C. Strumia, C.I. Alvarez Igarzabal, New hydrogel obtained from a novel dendritic monomer as a promising candidate for biomedical application, J. Biomed. Mat. Res. Part A 101 (2013) 3372–3381.
[27] G.R. Newkome, C.D. Weis, Di-*tert*-butyl 4-[(2-*tert*-butoxycarbonyl)ethyl]-4-aminoheptanedicarboxylate, Org. Prep. Proced. Int. 28 (1996) 495–498.
[28] Ciprofloxacin monograph in: RxList, The Internet Drug List. Web site: http://www.rxlist.com/script/main/srchcont_rxlist.asp?src=ciprofloxacin&x=39&y=14 (accessed on March 26th 2015).

[29] C.S. Fallati, A.A. Ahumada, R.H. Manzo, El perfil de solubilidad de la Ciprofloxacina en función del pH, Acta Farm. Bonaer. 13 (1994) 73–77.
[30] J.C. Cuggino, M. Calderón, C.I. Alvarez, M.C. Strumia, K.N. Silva, E.K. Penott-Chang, A.J. Müller, New dendronized polymers from acrylate Behera amine and their ability to produce visco-elastic structured fluids when mixed with CTAT worm-like micelles, J. Colloid Interface Sci. 357 (2011) 147–156.
[31] P.L. Páez, M.C. Becerra, I. Albesa, Chloramphenicol-induced oxidative stress in human neutrophils, Basic Clin. Pharmacol. Toxicol. 103 (2008) 349–353.
[32] S. Wang, H. Yu, J.K. Wickliffe, Limitation of the MTT and XTT assays for measuring cell viability due to superoxide formation induced by nano-scale TiO2, Toxicol. in Vitro 25 (2011) 2147–2151.
[33] International standards ISO 10993-5, Biological Evaluation of Medical Devices. Part 5: Tests for *In Vitro* Cytotoxicity, third ed., 2009.
[34] G. Ciapetti, E. Cenni, L. Pratelli, A. Pizzoferrato, *In vitro* evaluation of cell/biomaterial interaction by MTT assay, Biomaterials 14 (1993) 359–364.
[35] T. Higuchi, Rate of release of medicaments from ointment bases containing drugs in suspension, J. Pharm. Sci. 50 (1961) 874–875.
[36] Food and Drug Administration, Guidance for industry dissolution testing of immediate release solid oral dosage formsWeb site: http://www.fda.gov/Drugs/GuidanceComplianceRegulatoryInformation/Guidances/ucm200707.html (accessed on May 22, 2016).
[37] Farmacopea Argentina, 7ma. Edición. Comisión Permanente para la Farmacopea Argentina. Ministerio de Salud de la Nación. ArgentinaWeb site: http://www.anmat.gov.ar/webanmat/fna/pfds/Farmacopea_Argentina_2013_Ed.7.pdf (accessed on December 17, 2014).
[38] USP30-NF25, The United States Pharmacopeia–The National Formulary, The United States Pharmacopeial Convention, Inc., Rockville MD, 2007.
[39] J. Draize, G. Woodard, H. Calvery, Methods for the study of irritation and toxicity of substances topically applied to skin and mucous membranes, J. Pharmacol. Exp. Ther. 82 (1944) 377–390.
[40] Productos Higiénicos Descartables de Uso Externo e Intravaginal, Resolución MSyAS N° 288/90. Ministerio de Salud y Acción Social de la NaciónWeb site: www.anmat.gov.ar/inspectores/normativa/Resolucion_288_90.pdf (accessed on January 01, 2015).
[41] Carbopol 974P: Safety data sheet. The Lubrizol CorporationWeb site: https://www.lubrizol.com/LifeScience/Products/Carbopol/Carbopol-974P-NF.html (accessed on May 22, 2016).
[42] R. Nagalapalli, S.Y. Bheem, Synthesis, crystal structure, and Hirshfeld surface analysis of ciprofloxacin-salicylic acid molecular salt, Journal of Crystallography (2014) 1–5, http://dx.doi.org/10.1155/2014/936174 (Hindawi Publishing Corporation).
[43] K.J. Paluch, T. McCabe, H. Müller-Bunz, O.I. Corrigan, A.M. Healy, L. Tajber, Formation and physicochemical properties of crystalline and amorphous salts with different stoichiometries formed between ciprofloxacin and succinic acid, Mol. Pharm. 10 (10) (2013) 3640–3654.
[44] S. Pandey, P. Pandey, G. Tiwari, R. Tiwari, A.K. Rai, FTIR spectroscopy: a tool for quantitative analysis of ciprofloxacin in tablets, Indian J. Pharm. Sci. 74 (1) (2012) 86–90.
[45] M. Barón, IUPAC definitions of basic terms relating to low-molar-mass and polymer liquid crystal, Pure Appl. Chem. 73 (5) (2001) 845–895.
[46] N. Washington, C. Washington, C.G. Wilson, Transdermal Drug Delivery in: Physiological Pharmaceutics, Barrier to Drug Absorption, second ed. Taylor and Francis, NY, 2001 181–198.
[47] G. Bonacucina, S. Martelli, G.F. Palmieri, Rheological, mucoadhesive and release properties of Carbopol gels in hydrophilic cosolvents, Int. J. Pharm. 282 (2004) 115.
[48] C.H. Lee, V. Moturi, Y. Lee, Thixotropic property in pharmaceutical formulations, J. Control. Release 136 (2009) 88.
[49] A.F. Jimenez-Kairuz, D.A. Allemandi, R.H. Manzo, Equilibrium properties and mechanism of kinetic release of metoclopramide from carbomer hydrogels, Int. J. Pharm. 250 (2003) 129–136.
[50] A.P. Vilchez, A.F. Jimenez-Kairuz, F. Alovero, M.E. Olivera, D.A. Allemandi, R.H. Manzo, Release kinetics and up-take studies of model fluoroquinolones from carbomer hydrogels, Int. J. Pharm. 246 (2002) 17–24.
[51] R.C. Moellering Jr., The problem of complicated skin and skin structure infections: the need for new agents, J. Antimicrob. Chemother. 65 (Suppl. 4) (2010) iv3–iv8.
[52] M. Guggenheim, R. Zbinden, A.E. Handschin, A. Gohritz, M.A. Altintas, P. Giovanoli, Changes in bacterial isolates from burn wounds and their antibiograms: a 20-year study (1986–2005), Burns 35 (2009) 553–560.